Mixing Schemes and Liquid–Solid Phase Diagram in the Water-Rich Region of Aqueous 2-Butoxyethanol

Yoshikata KOGA,*,# Toshiaki TANAKA, Tooru ATAKE, Peter WESTH,†,## and Aase HVIDT†
Research Laboratory of Engineering Materials, Tokyo Institute of Technology, Nagatsuta, Midori-ku, Yokohama 227
† Department of Chemistry, University of Copenhagen, Copenhagen Ø, DK-2100, Denmark
(Received April 12, 1994)

Liquid–solid phase diagram was determined in the water-rich region of aqueous 2-butoxyethanol. A solid addition compound was suggested with the composition $x_{BE}^{add}=0.0260$, which melts incongruently at 269.5 K. The mixing scheme boundary separating two regions in the single liquid phase domain (*Chem. Phys. Lett.*, **217**, 245 (1994)) was found to cross the incongruent melting point of the above solid addition compound.

Recently, thermodynamic properties of aqueous 2-butoxyethanol (abbreviated as BE, hereinafter) have been investigated extensively.[1—9] In these works, the thermodynamic quantities proportional to the second derivatives of Gibbs free energy were measured directly, or calculated accurately. Using such data, it was found that there are three regions in the liquid single phase domain in the composition–temperature field, in each of which the mixing scheme is qualitatively different from those in the other regions. By mixing scheme, we simply mean the way in which the solute and solvent molecules mix with each other. The boundaries at 298.15 K, for example, are at $x_{BE}=0.0175$ and 0.5, where x_{BE} is the mole fraction of BE.

In the water-rich region (called region I), the solute molecule evidently introduce enhancement of the hydrogen bond network of water, consistent with the general notion of "iceberg formation".[10,11] BE–BE interaction were found to be characterized by enthalpic repulsion[5,7,8] and entropic attraction.[6] The magnitude of entropic effect, however, surpasses the enthalpic effect, resulting in net attraction in terms of Gibbs free energy,[6] hence the "hydrophobic attraction".[10,11] As the concentration of BE increases the enhancement of the hydrogen bond network of H_2O progresses gradually until the saturation point, $x_{BE}=0.0175$ at 298.15 K, beyond which a different mixing scheme sets in.[1,3—8]

In the intermediate region (II), $0.0175<x_{BE}<0.5$ at 298.15 K, two kinds of clusters appear to form rich in each component, naturally leading to phase separation with LCST.[12—14] The BE-rich clusters may be of micellar form, and the boundary between (I) and (II) may thus be analogous to the critical micelle composition. In Fig. 1, the boundary separating regions (I) and (II) is shown. It was drawn through the points at which anomalies were observed in various quantities that are proportional to the third derivatives of Gibbs free energy.[1,3—8]

In the BE-rich region (III), $x_{BE}>0.5$ at 298.15 K, the partial molar quantities indicated that BE molecules form clusters made purely of BE, and H_2O molecules interact as a single molecule with the surfaces of such clusters. The BE clusters could be in a micellar form.

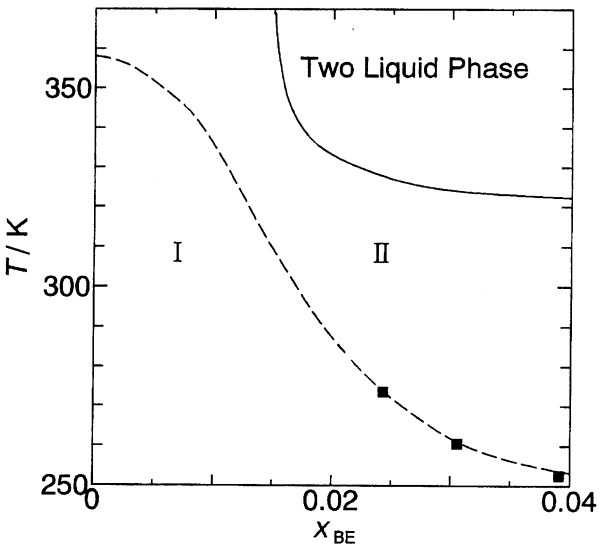

Fig. 1. The mixing scheme boundary separating regions (I) and (II). The broken line, the loci of anomalies in the third derivatives of Gibbs free energy, Refs. 1, 3, 4, 5, 6, 7, and 8. ■, the loci of step anomalies in $(\partial C_p/\partial T)$, this work.

Some dynamic properties have also been known to change across the mixing scheme boundary between (I) and (II). The hydrodynamic radii of diffusing species were found to be larger by two order of magnitude in region (I) than those in region (II).[15,16] The ionic and thermal conductivities change their slopes at the boundary.[17]

As shown in Fig. 1, the mixing scheme boundary ends at $x_{BE}=0$ and $T=358$ K. It was noted[3,7] that the hydrogen bond network loses its percolation at this temperature in pure H_2O. Namely, an estimate indicates that in pure H_2O the hydrogen bond probability decreases as temperature increases, and reaches about 0.37 at 358 K.[18] For a diamond structure (ice Ih), which is topologically the same in liquid water in terms of hydrogen bond connectivity, the percolation threshold is

#Center for Ceramics Research. Permanent address: Department of Chemistry, The University of British Columbia, Vancouver, B. C. Canada V6T 1Z1.
##Carlsberg Foundation Fellow.

known to be 0.39.[19] Hence, above 358 K, there is no percolation in the hydrogen bond network of H_2O, or the network does not extend throughout the entire bulk any longer. This implies, in turn, that the percolating hydrogen bond network in H_2O is prerequisite for the mixing scheme in region (I).

The present work concerns with the way in which the mixing boundary between (I) and (II) ends at low temperature. No doubt that the difference in mixing scheme in liquid mixture must manifest itself in the freezing behavior, i.e. liquid–solid phase diagram. There is a brief report on the phase diagram in literature.[12] However, it lacks in detail in the water-rich region.

First, we extended the mixing scheme boundary to lower temperature. We measured heat capacities, C_p, by differential scanning calorimetry (DSC) on cooling. Probably due to a small sample size (0.02 mL) the sample supercooled readily, and C_p data for liquid mixtures were obtained to about 240 K. From the temperature dependence of C_p, the loci of the mixing scheme boundary were obtained as described previously.[1] They are plotted in Fig. 1. Next, the temperature traces on heating or cooling, were recorded by means of classical DTA (differential thermal analysis). The classical DTA suits the present purpose in that it gives the accurate temperature of the sample at any given time.[20] It has been successfully applied to determine such a complicated liquid–solid phase diagram as Cu_2S–Bi_2S_3 system.[21]

Experimental

2-Butoxyethanol used were from Merck–Schuchardt for DSC and from Wako for DTA. H_2O was doubly distilled. The mixtures were made by weighing.

The heat capacities, C_p, of solutions were measured as a function of temperature by means of Perkin–Elmer (DSC 7) differential scanning calorimeter. The detail is described elsewhere.[22,23] Briefly, about 0.02 mL sample was cooled at a rate of 10 K min^{-1} to about 240 K. The difference in the heat flow to the sample and the reference pans was recorded. Thus, C_p data were calculated as function of temperature before freezing occurred. The uncertainty is estimated to be about 0.8%.

The heating or cooling curves of the mixtures were taken by means of a home-made classical DTA apparatus. The detail is described elsewhere.[24] Briefly, a sample of about 0.5 mL was placed in a 5 mm i.d. glass tube with a 1 mm o.d. thermocouple well at the center. The sample tube and the reference tube filled with α-Al_2O_3 were placed in the wells bored symetrically in a copper block of 38 mm in diameter and 70 mm in hight. The copper block was cooled or heated at a rate from 1 to 3 K min^{-1}. The temperature of the copper block, i.e. the surrounding of the sample was monitored by the temperature of the reference cell. A modification was made to the original set-up in that the EMF data from two thermocouples, one from the temperature of the reference cell and the other for the temperature difference between the sample and reference cells were fed to digital voltmeters (Hewlett–Packard 3748A, and Advantest TR-6856). The digitized signals were then fed to a PC through an IEEE-488 interface. Thus, the actual temperature of the sample was calculated as a function of time. The heating curve of pure H_2O indicated the melting occurred from 273.1 to 273.2 K. Therefore, the uncertainty due to thermal conduction or lack of it in the system is estimated as better than ±0.1 K.

Results and Discussion

Figure 2 shows the C_p data for $x_{BE}>0.02$ as a function of T determined by DSC. In the previous paper,[1] C_p data by high precision DSC were reported for $x_{BE}<0.02$. It was pointed out that the temperature derivative, $(\partial C_p/\partial T)$, a third derivative of Gibbs free energy showed a weak jump anomaly. Or equivalently, the curve C_p vs. T showed a clear bend at the same locus. The loci of such anomalies fell on the mixing scheme boundary shown in Fig. 1. From the data in Fig. 2, we located such anomalies within ±1 K and plotted in Fig. 1. As is evident in Fig. 1, the mixing scheme boundary for $x_{BE}<0.02$ extends smoothly into a possibly super-cooled region, $x_{BE}>0.02$.

Figure 3 shows a typical cooling curve. A substantial supercooling is evident, and freezing occurred at 256 K, while the equilibrium freezing point seemed to be about 270 K for this solution. The subsequent heating curve shown in Fig. 4 indicates the melting started at 269.1 K and ended at 269.8 K.

All the melting points on heating are listed in Table 1. The uncertainty due to thermal conduction or the lack of it was estimated as less than ±0.1 K above. However, there is another important source of uncertainty. Namely, since there is no forced mixing in the cell, the composition may not be homogeneous throughout. Figure 5 shows the temperature trace of the sample, T_s, when heating was reversed to cooling at an early stage

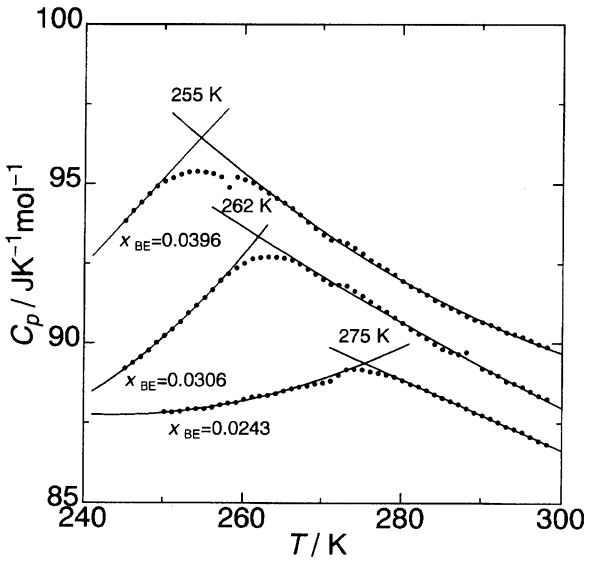

Fig. 2. Heat capacities of aqueous 2-butoxyethanol measured by DSC. x_{BE} is the mole fraction of 2-butoxyethanol. The uncertainty is about 0.8%.

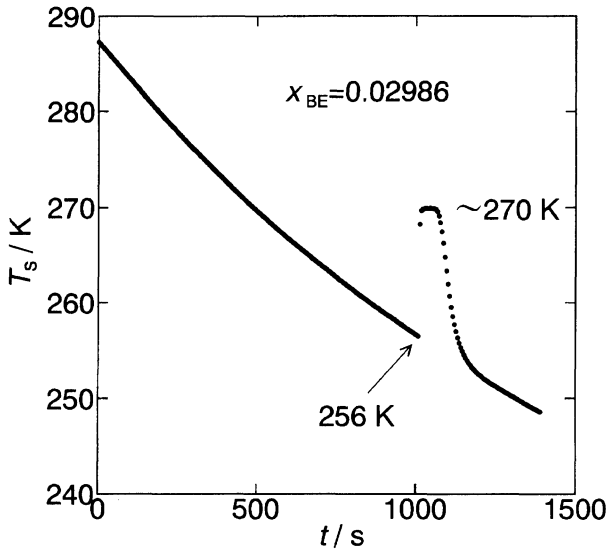

Fig. 3. The cooling curve of aqueous 2-butoxyethanol, $x_{BE}=0.02986$. The temperature of the sample, T_s, against time.

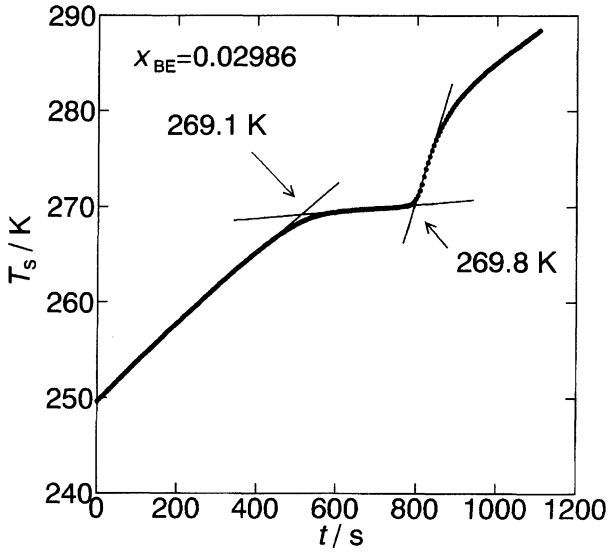

Fig. 4. The heating curve of aqueous 2-butoxyethanol $x_{BE}=0.02986$. The temperature of the sample, T_s, against time.

of melting. Note, in Fig. 5, the temperature trace, T_r, of the reference cell, which indicates the reversal to cooling from heating. Since there were some solid nuclei present which prevented supercooling, the end point of freezing could be determined. If the true equilibrium exists the starting point of melting and the end point of freezing should be identical. Figure 5 indicates the end of freezing to be 269.8 K for $x_{BE}=0.02603$, which is to be compared with 269.3 and 269.4 K as the starting point of melting. (See Table 1.) This discrepancy may reflect the lack of mass transfer and the better value is likely to be $(269.3+269.8)/2=269.6$ K. Hence, the values listed in Table 1 may have to be corrected for by +0.2 K. All in all, it may be safe to say the melting points are the values in Table 1 with uncertainty ±0.3 K for the absolute values. On the other hand, the uncertainty relative to those of other composition should remain to be better than ±0.1 K. For mixtures, $x_{BE}>0.4$, glass appeared to form rather than solid on cooling, and this will be a subject of a future study. The melting points listed in Table 1 are plotted in Fig. 6 for $x_{BE}<0.1$ and Fig. 7 for $x_{BE}<0.5$.

Table 1. Melting Points of the Mixtures BE–H_2O

x_{BE}	Beginning	End
	K	K
0	273.1	273.2
0.004692	269.5	272.6
0.01027	269.4	272.2
0.01027	269.5	272.0
0.01818	269.5	271.0
0.01950	296.5	270.4
0.02031	269.4	270.5
0.02031	269.5	270.5
0.02238	269.3	270.2
0.02406	269.3	270.2
0.02603	269.4	270.2
0.02603	269.3	270.3
0.02793	269.4	270.0
0.02986	269.0	269.5
0.02986	269.1	269.8
0.03873	268.7	269.5
0.06018	268.0	269.5
0.07940	267.6	269.5
0.09779	267.5	269.4
0.09779	267.5	269.4
0.1992	264.4	267.5
0.3024	257.6	265.8
0.3948	251.5	260.5
0.4886	Glass	

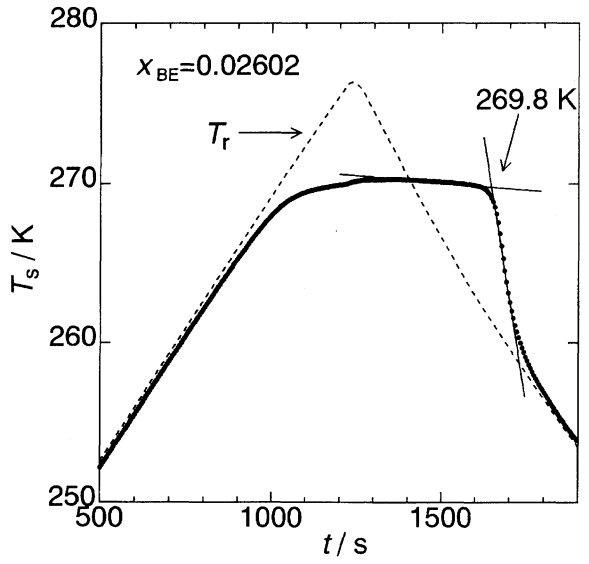

Fig. 5. The temperature trace of aqueous 2-butoxyethanol, $x_{BE}=0.02602$. The broken line is the temperature trace of the reference, T_r, i.e. the surrounding of the sample, see the text.

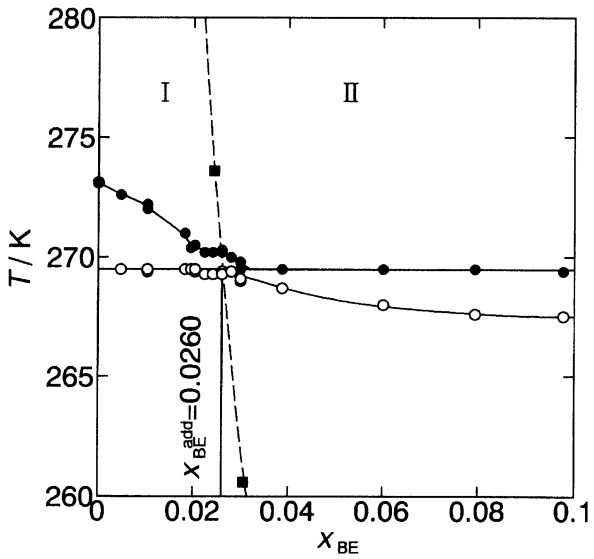

Fig. 6. The solid–liquid phase diagram of aqueous 2-butoxyethanol, for $x_{BE}<0.1$. The broken line is the mixing scheme boundary, as shown in Fig. 1. ○; the beginning of melting. ●; the end of melting. See Table 1.

It is evident from Figs. 6 and 7 that, for $x_{BE}>0.026$, the solution freezes into a solid solution, while for $x_{BE}<0.03$ the mixture freezes with an eutectic at 269.5 K. To be consistent with Gibbs' phase rule, there should exists a solid addition compound with the composition $x_{BE}^{add}=0.0260$. The phase diagram indicates that this addition compound melts incongruently. What is striking is that the mixing scheme boundary separating liquid regions (I) and (II) cross the incongruent melting point 269.5 K of this addition compound. Thus, the species of the form $BE(H_2O)_n$, which was suggested to exist in solution,[14,25] while its actual existence in liquid mixture is debatable,[3,5—8] does indeed exist as the solid addition compound.

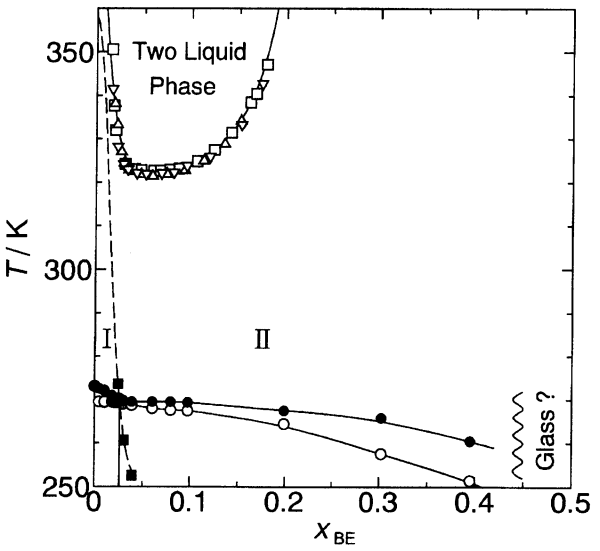

Fig. 7. The phase diagram of aqueous 2-butoxyethanol, for $x_{BE}<0.5$. The broken line is the mixing scheme boundary. ○; the beginning of melting. ●; the end of melting. See Table 1.

Two additional features are noteworthy in the phase diagram. At about $0.022<x_{BE}<0.026$, the liquidus curve shows a rather flat portion, beyond the relative uncertainty, ±0.1 K. This implies that the concentration fluctuation in the liquid phase at about 271 K should be large.[26,27] In the range $0.03<x_{BE}<0.08$, the liquidus curve is also flat. This could similarly imply that the concentration fluctuation of liquid of the composition in this range and at temperatures close to the freezing points, 269.5 K, must also be large. When the temperature was raised from room temperature to that of LCST, the light scattering studies showed an increase in the concentration fluctuation approaching the flat portion of the two liquid phase separation.[14,28] Similar observation may be expected when the temperature is lowered to the flat portion of the liquidus curve.

We conclude that the mixing scheme boundary between liquid regions (I) and (II) leads to the solid addition compound, $x_{BE}^{add}=0.0260$, at its incongruent melting point, 269.5 K.

This research was supported by Ministry of Education, Science and Culture, Japan, the Carlsberg Foundation, Denmark, and NATO Collaborative Research Program. The guest professorship for one of us (Y. K) at the Center of Ceramics Research, Research Laboratory of Engineering Materials, Tokyo Institute of Technology was financed by Ministry of Education, Science and Culture, Japan. We thank Mr. Takeshi Mizutani for drawing our attention to Ref. 21, and for various technical assistance.

References

1) P. Westh, Aa. Hvidt, and Y. Koga, *Chem. Phys. Lett.*, **217**, 245 (1994).
2) Y. Koga, J. Kristiansen, and Aa. Hvidt, *J. Chem. Thermodyn.*, **25**, 51 (1993).
3) Y. Koga, *J. Phys. Chem.*, **96**, 10466 (1992).
4) J. V. Davies, F. W. Lau, L. T. N. Le, J. T. W. Lai, and Y. Koga, *Can. J. Chem.*, **70**, 2659 (1992).
5) W. W. Y. Siu, T. Y. H. Wong, J. T. W. Lai, A. Chong, and Y. Koga, *J. Chem. Thermodyn.*, **24**, 159 (1992).
6) Y. Koga, *J. Phys. Chem.*, **95**, 4119 (1991).
7) Y. Koga, W. W. Y. Siu, and T. Y. H. Wong, *J. Phys. Chem.*, **94**, 3879 (1990).
8) W. Siu and Y. Koga, *Can. J. Chem.*, **67**, 671 (1989).
9) Aa. Hvidt and Y. Koga, *Thermochim. Acta*, **228**, 39 (1993).
10) F. Franks and J. E. Ives, *Q. Rev., Chem. Soc.*, **20**, 1 (1966).
11) F. Franks and J. E. Desnoyers in "Water Science Review," ed by F. Franks, Cambridge Univ. Press., Cambridge (1985), Vol. 1, p. 171.
12) F. Quirion, L. J. Magid, and M. Drifford, *Langmuir*, **6**, 244 (1990).

13) C. M. Ellis, *J. Chem. Educ.*, **44**, 405 (1967).
14) N. Ito, T. Fujiyama, and Y. Udagawa, *Bull. Chem. Soc. Jpn.*, **56**, 379 (1983).
15) S. Kato, D. Jobe, N. P. Rao, C. H. Ho, and R. E. Verral, *J. Phys. Chem.*, **90**, 4167 (1986).
16) T. M. Bender and P. Pecora, *J. Phys. Chem.*, **92**, 1675 (1988).
17) K. T. Puhacz, C. C. M. Hui, Y. Ootsuka, H. Kawaji, T. Atake, and Y. Koga, *Rep. Res. Lab. Eng. Mater., Tokyo. Inst. Technol.*, **19**, 263 (1994).
18) H. E. Stanley and J. Teixeira, *J. Chem. Phys.*, **73**, 3404 (1980).
19) N. G. Parsonage and L. A. K. Staveley, in "Disorder in Crystals," Clarendon, Oxford (1978), p. 84.
20) K. Saito, T. Atake, and Y. Saito, *Netsu Sokutei*, (*Calorimetry and Thermal Analysis*), **14**, 2 (1987).
21) A. Sugaki and H. Shima, *Tech. Rep. Yamaguchi Univ.*, **1**, 45 (1972).
22) P. Westh and Aa. Hvidt, *Biophys. Chem.*, **46**, 27 (1993).
23) P. Westh, *J. Phys. Chem.*, **98**, 3222 (1994).
24) T. Atake, A. Hamano, and Y. Saito, *Thermochim. Acta*, **109**, 267 (1986).
25) Aa. Hvidt, *Ann. Rev. Biophys. Bioeng.*, **12**, 1 (1983).
26) A. B. Bhatia and N. H. March, *Phys. Lett. A*, **41A**, 397 (1972).
27) A. B. Bhatia and N. H. March, *J. Phys. F*, **F5**, 1100 (1975).
28) T. Kato, *J. Phys. Chem.*, **89**, 5750 (1985).